2011 American Control Conference
on O'Farrell Street, San Francisco, CA, USA
June 29 - July 01, 2011

Root Locus Design with Complex Proportional-Integral-Lead Compensation

Qi Zhang, William C. Messner

Abstract— **The Complex Proportional-Integral-Lead (CPIL) compensator is a relatively new compensator structure that is a variation of the commonly used PI-lead compensator. The complex conjugate zeros provide additional design flexibility compared with the standard structure. Until now, the potential of the CPIL has only been examined for controller design via frequency response. This paper examines the utility of the CPIL for root locus design. We illustrate two design strategies by considering compensator design for a double integrator and for a second order system with a very lightly damped resonance.**

I. INTRODUCTION

The complex Proportional-Integral-Lead (CPIL) compensator was introduced in [1]. The CPIL compensator is a variation of the commonly used PI-lead compensator (see for example [2]), which is the cascade of a PI compensator and a first-order lead compensator. The CPIL has one pole at the origin and one negative real pole, but its zeros can appear in complex conjugate pairs. Selection of the damping ratio of the zeros of the CPIL provides additional design flexibility compared to the standard PI-lead. While others have employed damping ratios less than one for Proportional-Integral-Derivative (PID) compensators, a close relative of the CPIL, their work has specifically addressed gain compensation rather than phase compensation (see for example [3]). Until now, the potential of the CPIL compensator has only been examined for frequency response controller design [4], [5].

This paper analyses the utility of the CPIL for root locus design and illustrates two design strategies. In the first strategy, we specify the desired overshoot and settling time and determine corresponding dominant desired closed-loop second-order poles [6], [7]. We then determine the CPIL compensator providing (1) the angle contribution at those locations in the complex plane so that those desired poles are on the root locus and (2) the correct gain. As is common for this strategy, the assumption that the second-order poles are dominant is often not entirely accurate. The version of CPIL compensator presented here provides *two* design parameters – the damping ratio of the zeros and the relative angle contribution of the poles and zeros – that can be manipulated to achieve the specifications or at least improve the result. Prior work only examined the effect of the damping ratio of the zeros.

In the second design strategy, we specify the angle of departure of two lightly damped open-loop complex conjugate poles, and we manipulate the design parameters of the CPIL to optimize the controller effort, overshoot, and settling time for these specific departure angles. We then search over the space of departure angles to find the best CPIL design.

This paper is organized as follows. Section II reviews the CPIL compensator and its design parameters. Section III presents the application of the strategy of dominant second-order poles to a double integrator, Section IV the strategy of optimal angle of departure second order system with a very lightly damped resonance. Section V contains concluding remarks.

II. CPIL COMPENSATOR REVIEW

Consider the point $-u+jv$ in the second quadrant of the complex plan (i.e., $u>0$ and $v>0$). The following generalized CPIL compensator

$$C_{cpil}(s)=\frac{(s+u)^2+2\zeta\omega_z(s+u)+\omega_z^2}{s(s+u+p)} \tag{1}$$

contributes phase angle

$$\phi_{cpil}\equiv\angle C_{cpil}(u+jv)=\frac{3}{2}\phi_m-45^\circ-\arctan\left(\frac{u}{v}\right) \tag{2}$$

at $-u+jv$, when

$$\omega_z=v\left(-\zeta\tan(\phi_m-\delta)+\sqrt{\zeta^2\tan^2(\phi_m-\delta)+1}\right), \tag{3}$$

and

$$p=v\left(\frac{1+\sin(\phi_m+2\delta)}{\cos(\phi_m+2\delta)}\right), \tag{4}$$

for $\zeta>0$ and

$$\begin{aligned}-90^\circ<\phi_m-\delta<90^\circ\\ -90^\circ<\phi_m+2\delta<90^\circ.\end{aligned} \tag{5}$$

Note that the last two relations imply that $-90^\circ<\phi_m<90^\circ$.

The phase contribution of the components of the compensator are the following.

- The pole at the origin is $-90^\circ-\arctan(u/v)$.
- The pole at $-(u+p)$ contributes $\phi_m/2+\delta-45^\circ$.
- The two zeros contribute a total of $\phi_m-\delta+90^\circ$.

Note that the parameters ζ and δ do not affect the angle contribution and serve as design variables for the control engineer, provided they lie within certain limits. The parameter δ specifies the relative phase contribution of the poles and zeros, and has not been addressed in earlier work. The damping ratio ζ can be greater than 1.

W. Messner is with Department of Mechanical Engineering, Carnegie Mellon University, 5000 Forbes Avenue, Pittsburgh, Pennsylvania, USA

Q. Zhang is with Department of Mechanical Engineering, RWTH Aachen University, Templergraben 55, 52062 Aachen, Germany

The limits on the selection of δ imply that

$$\delta_{min} = \begin{cases} -\left(45^\circ + \frac{\phi_m}{2}\right) & \text{for } -90^\circ < \phi_m < -30^\circ \\ \phi_m - 90^\circ & \text{for } 30^\circ \le \phi_m < 90^\circ \end{cases} \quad (6)$$

$$\delta_{max} = \begin{cases} \phi_m + 90^\circ & \text{for } -90^\circ < \phi_m < -30^\circ \\ 45^\circ - \frac{\phi_m}{2} & \text{for } -30^\circ \le \phi_m < 90^\circ \end{cases}. \quad (7)$$

To simplify the designer's job, we introduce the parameter $-1 < \alpha < 1$ which specifies δ as follows

$$\delta = \begin{cases} -\alpha\delta_{min} & \text{for } \alpha < 0 \\ \alpha\delta_{max} & \text{for } \alpha > 0 \end{cases}. \quad (8)$$

III. DESIGN FOR DOMINANT POLES

To illustrate root locus design for dominant second-order poles with the CPIL compensator, we consider a double integrator plant with transfer function

$$P(s) = \frac{1}{s^2}. \quad (9)$$

Our closed-loop performance specifications are

- zero steady-state error for a constant input disturbance
- 20% overshoot
- 2% setting time of 3 *sec*.

The first specification implies the need for integral control. The corresponding dominant second-order poles for the overshoot and settling time specifications are $p_{des} = -u \pm vj$ where $u = 1.3333$ and $v = 2.6026$. Since

$$\angle P(-1.333 + 2.603j) = -234.3^\circ \quad (10)$$

the CPIL compensator must contribute $\phi_{cpil} = 54.3^\circ$ at $-u + vj$.

To use the CPIL compensator, we must first determine ϕ_m from (2)

$$\phi_m = \frac{2}{3}\left(\phi_{cpil} + \arctan\left(\frac{u}{v}\right)\right) + 30^\circ. \quad (11)$$

Evaluating this expression gives $\phi_m = 84.3^\circ$.

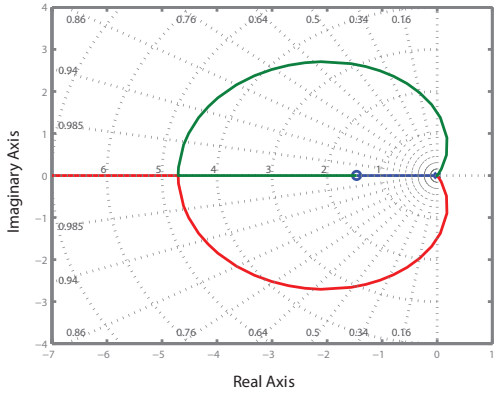

Fig. 1. Root locus of $P(s)C_{PIL}(s)$

We begin the design iteration process by considering the case of $\alpha = 0$ and $\zeta = 1$, which gives a standard PIL with a double real zero. Subsequently, we will vary both of these parameters to observe the effect on the root locus and on the closed loop. Applying (1)-(4) $\alpha = 0$ and $\zeta = 1$ leads to

$$C_{PIL} = \frac{s^2 + 2.928s + 2.143}{s(s + 53.18)} \quad (12)$$

which has two zeros at -1.464. Fig. 1 shows the root locus of $P(s)C_{PIL}(s)$. The gain corresponding to the desired dominant poles is $K = 191$. The two remaining closed-loop poles for this gain are 0.967 and -49.4.

Fig. 2 shows the step response of the closed-loop system. The settling time is 2.6 seconds, but the zeros at -1.464 lead to an excessive overshoot of 39%.

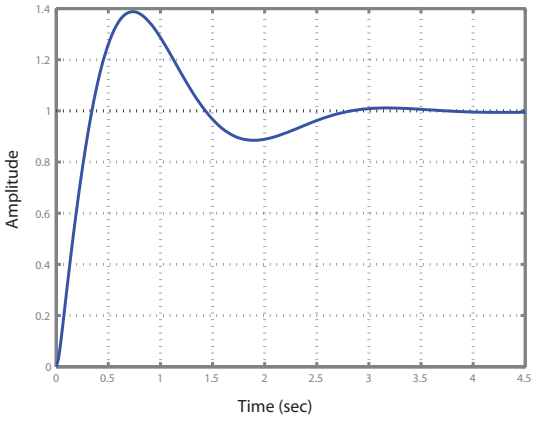

Fig. 2. Step response of $G_{CL,PIL}$

The controller effort is another important quantity. The closed-loop transfer function from reference to controller effort is

$$\frac{U(s)}{R(s)} = \frac{KC(s)}{1 + KP(s)C(s)}. \quad (13)$$

Fig. 3 shows that for the controller (12) and gain $K = 191$ the maximum controller effort is 191.

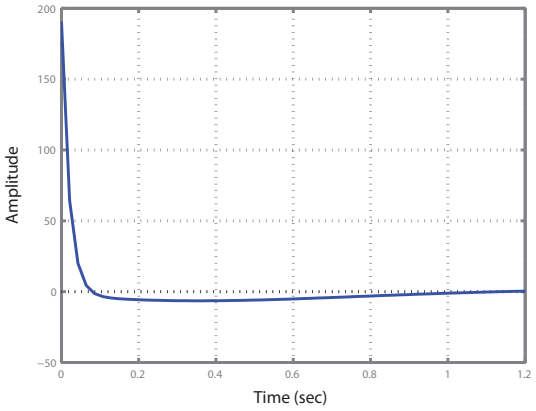

Fig. 3. Controller effort of $G_{CL,PIL}$

To improve the overshoot and controller effort, we adjust the parameter α in the range [-0.9 to 0.9] and ζ in the range [0.3 to 1.7]. Fig. 4 shows the effect of α and ζ on the overshoot. Increasing α decreases the overshoot slightly while ζ has little effect.

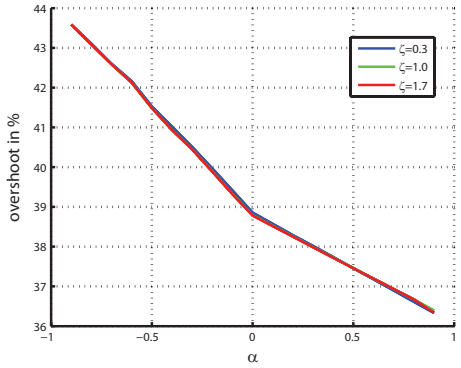

Fig. 4. Overshoot as a function of α for several damping ratios

Fig. 5 shows that all values of α and ζ satisfy the the settling time specification. Settling time decreases slightly with increasing α, and for relatively large α decreasing the damping ratio also decreases the settling time slightly.

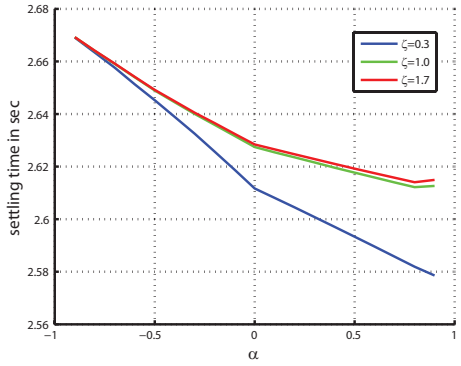

Fig. 5. Settling time as a function of α for several damping ratios

The parameter α has its biggest effect on the maximum controller effort (Fig. 6). Again, the effect of ζ is very small, but the controller effort increases with increases rapidly with α.

The results of this analysis suggest that the primary optimization is trading off the effect of α on the overshoot and controller effort, since the settling time specification is achieved and ζ has only a minor effect on the quantities of interest.

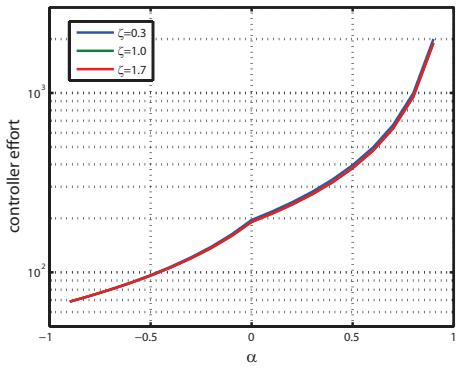

Fig. 6. Maximum controller effort of α for several damping ratios

Fig. 7 shows some root loci of $P(s)C_{PIL}(s)$, including the locations of the desired closed-loop poles, for different αs and ζs. For $\alpha = -0.9$, the root loci are "open", while the root loci are "closed" for $\alpha = 0$ and $\alpha = 0.9$. For $\zeta < 1$ the loci contain two complex conjugate zeros, $\zeta = 1$ leads to a double real zero, and zeros for $\zeta > 1$ yields two distinct real zeros.

IV. DESIGN FOR ANGLE OF DEPARTURE

To illustrate root locus design for optimal angle of departure, we consider the second order plant transfer function

$$P(s) = \frac{1}{s^2+1}. \tag{14}$$

The closed-loop performance specifications are

- zero steady-state error for a constant input disturbance
- closed-loop damping ratio greater than than 0.5
- 2% settling time less than 8 seconds
- controller effort less than 4 times the minimum.

To guarantee stability, we first specify an angle of departure ϕ_{dep} at the pole $p_a = j$ to point into the left-half plane (LHP). Given ϕ_{dep}, we then can calculate the phase ϕ_{cpil} that the CPIL compensator must contribute using

$$\phi_{cpil} = -180^\circ + \sum_k \angle(p_a - p_k) - \sum_l \angle(p_a - z_l) + \phi_{dep}. \tag{15}$$

Since any angle of departure in the range 90° to 270° points into the LHP, we specify the angle of departure in this range. Our initial choice of ϕ_{dep} is 120°, which leads to $\phi_{cpil} = 30^\circ$ at p_a from (15). Applying (11) gives $\phi_m = 50^\circ$.

Again, we begin the design iteration process by considering the case of $\alpha = 0$ and $\zeta = 1$, which leads to

$$C_{PIL} = \frac{s^2 + 0.7279s + 0.1325}{s^2 + 2.747s}. \tag{16}$$

Fig. 8 shows the root locus of $P(s)C_{PIL}(s)$. Since a closed-loop damping ratio ζ_{CL} higher than 0.5 is desired, we determine the maximum closed-loop damping ratio, which is $\zeta_{CL} = 0.30$. The corresponding gain is $K = 6$, giving the four closed-loop poles $-0.159, -0.922$, and $-0.833 \pm 2.891j$.

Fig. 9 shows the step response of the closed-loop system. The settling time is 25 seconds and the overshoot is 19%. Fig. 12 shows that the maximum control effort is 6.

To improve overshoot and to meet the given specifications, we vary both α and ζ to observe their effects on the root locus and on the closed-loop. We adjust α in the range of [-0.9 to 0.9] and ζ in the range of [0.3 to 1.7].

Fig. 10 shows the effect of α and ζ on the closed-loop damping ratio ζ_{CL}. For $\zeta \geq 0.7$, the closed-loop damping ratio increases with increasing α and decreasing ζ. However, for $\zeta = 0.3$, the closed-loop damping ratio reaches a maximum of 0.59 at $\alpha = 0.2$. (The shaded area indicates the region where the corresponding specification is not met.) Fig. 10 shows that any design with $\zeta \geq 0.7$ and $\alpha \geq 0.45$ satisfies the closed-loop damping ratio specification. Alternatively, designs with $\zeta = 0.3$ and $0.05 \leq \alpha \leq 0.3$ satisfy the closed-loop damping ratio specification.

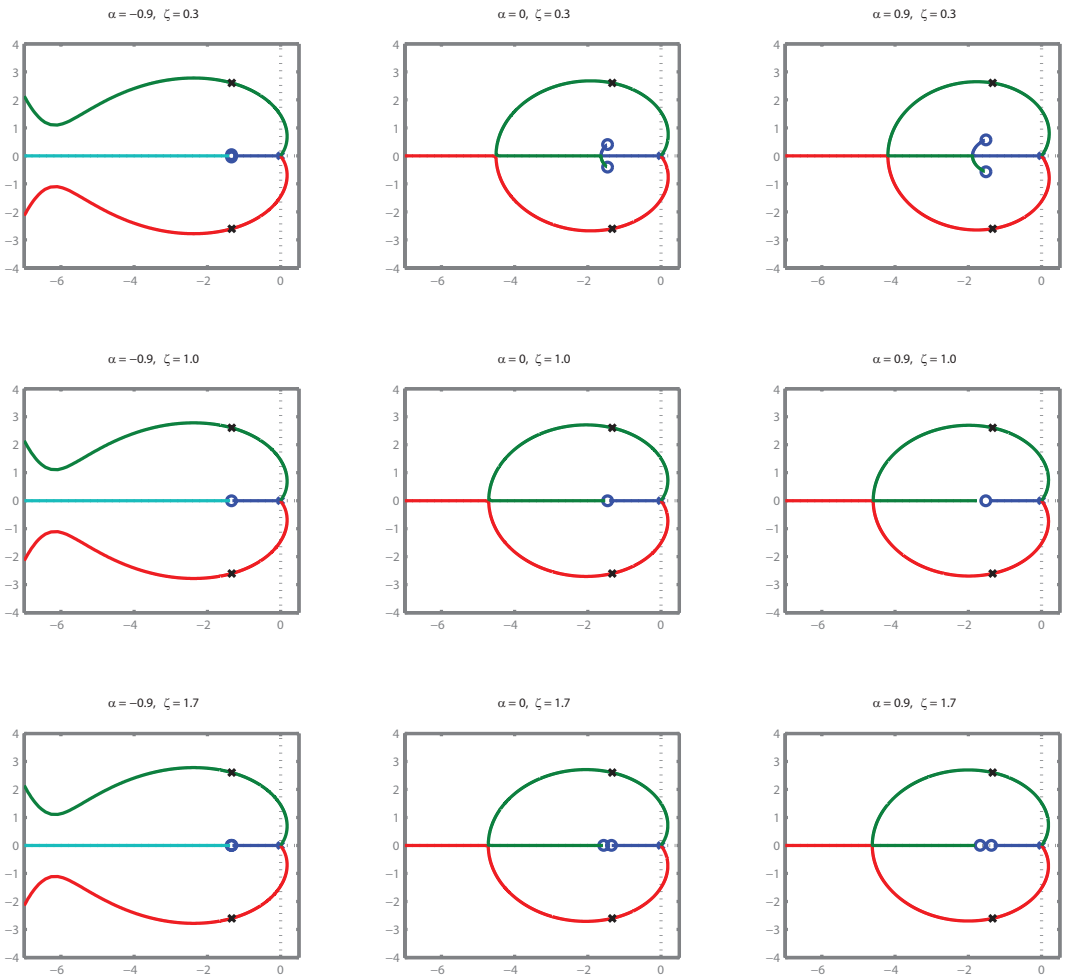

Fig. 7. Root loci for different αs and ζs

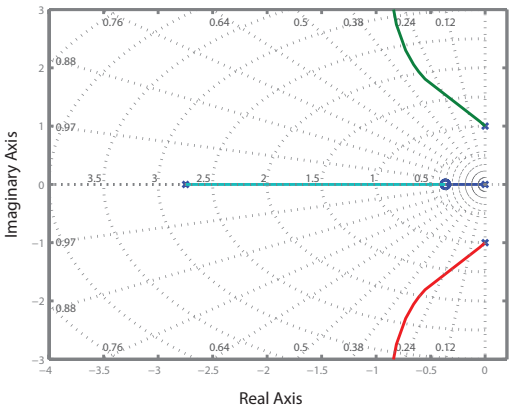

Fig. 8. Root locus of $P(s)C_{PIL}(s)$

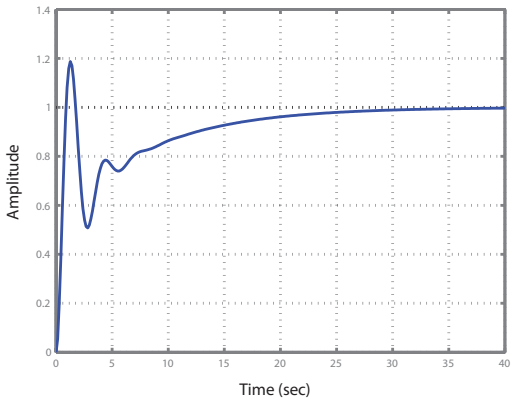

Fig. 9. Step response of $G_{CL,PIL}$

Fig. 11 shows the effect of α and ζ on the overshoot. The overshoot behaves differently for $\zeta = 0.3$ than for greater values. For comparison, we achieve an overshoot of 7% with $\alpha = 0.2$ and $\zeta = 0.3$, but 18% with the same α and $\zeta = 0.7$.

The controller effort increases rapidly with α (Fig. 13) while ζ only has a minor effect. The minimum of the maximum controller effort value is 2, and thus the maximum controller effort should not exceed 8 in the final design. Using $\zeta = 0.3$ and $\alpha < 0.35$ satisfies the maximum controller effort specification. Using $\zeta \geq 0.7$ and $\alpha < 0.2$ also satisfies this specification.

Fig. 14 shows that the parameter α has a big effect on the settling time, which decreases with increasing α. Larger values of ζ also decrease the settling time. Only $\zeta = 0.3$ and

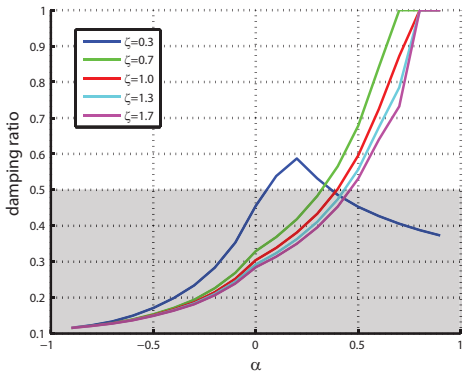

Fig. 10. Closed-loop damping ratio as a function of α for several values of ζ

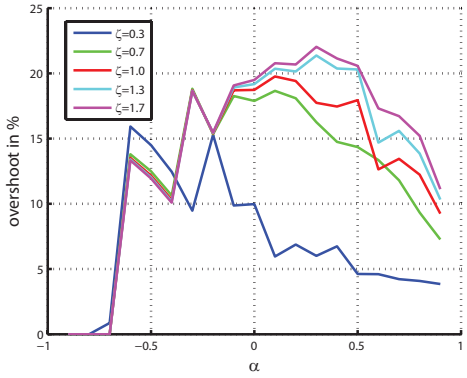

Fig. 11. Overshoot as a function of α for several damping ratios

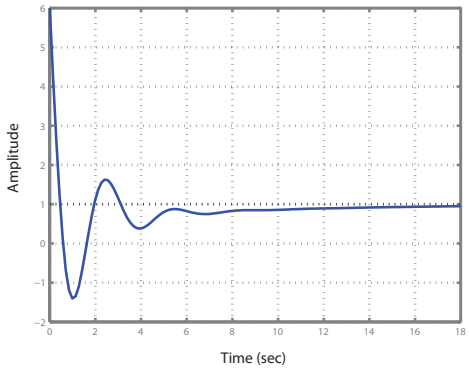

Fig. 12. Controller effort of $G_{CL,PIL}$

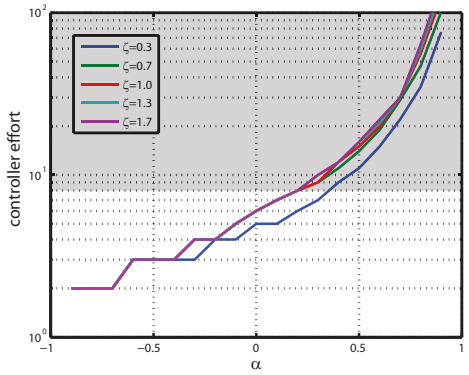

Fig. 13. Maximum controller effort of α for several damping ratios

$\alpha > 0.05$ and $\zeta = 0.7$ with $\alpha > 0.7$ satisfy the closed-loop settling time specification.

Based on the performance specification and the percent overshoot performance, the best design uses $\zeta = 0.3$ and $\alpha = 0.15$ for an angle of departure of 120°. Fig. 15 shows the root locus of $P(s)C_{CPIL}(s)$ that is constructed with those parameters. Fig. 16 shows the step response of the closed-loop system.

Next we examine the effect of the angle of departure ϕ_{dep} on the closed-loop response. Since, compared to α, ζ seems only to have a minor impact on the closed-loop, we choose ζ to be 0.3 and vary α and ϕ_{dep}.

Fig. 17 shows that the closed-loop damping ratio ζ_{CL} increases with increasing ϕ_{dep}. For $\phi_{dep} \geq 170°$, ζ_{CL} even becomes 1 for a big range of α. The effect of ϕ_{dep} on the overshoot is shown in Fig. 18. The overshoot decreases with increasing ϕ_{dep} until it reaches 0, which corresponds to $\zeta_{CL} = 1$. Both the controller effort (Fig. 19) and settling time (Fig. 20) increase with increasing ϕ_{dep}. The trade-off is that increasing ϕ_{dep} decreases overshoot while increasing controller effort and settling time.

V. CONCLUSION

This paper examined the utility of the CPIL for root locus design. In that respect, two design strategies, namely the design for dominant second-order poles and the design for optimal angle of departure, were illustrated.

The two parameters of the CPIL ζ and α can serve as design variables for the control engineer. In this work, their influence on the root locus and the closed-loop response was analysed. The results show that the usage of those design variables leads to higher flexibility of the CPIL and potentially, depending on the desired specifications, to significantly better closed-loop properties.

REFERENCES

[1] W. Messner, "Classical Controls Revisited", in *Proc. Proceedings of the 2008 Advanced Motion Controls Conference*, Trento, Italy, March 2008.

[2] T. Asumi, T. Arisaka, T. Shimizu, and T. Yamaguchi, "Vibration servo control design for mechanical resonant modes of a hard-disk-drive actuator" *JSME International Journal*, vol. 46, no. 3, Feb 2003, pp. 819-827.

[3] D. Abramovitch, S. Hoen, and R. Workman, "Semi-Automatic Tuning of PID Gains for Atomic Force Microscopes", in *Proc. 2008 American Control Conf.*, Seattle, WA, 11-13 June 2000, pp. 26842689.

[4] W. Messner, M. Bedillion, L. Xia, and D. Karns, "Lead and lag compensators with complex poles and zeros: design formulas for modeling and loop shaping", *IEEE Control Systems Magazine*, vol. 27, no. 1, Feb 2007, pp. 44-54.

[5] W. Messner, "Classical Control Revisited: Variations on a Theme", *Proceedings 10th International Workshop on Advanced Motion Control*, Trento, Italy, Mar 2008, pp. 15-20.

[6] G.F. Franklin, J.D. Powell, and A. Emani-Naeini, *Feedback Control of Dynamic Systems*. Prentice-Hall, Upper Saddle River, New Jersey, Fourth edition, 2002.

[7] N.S. Nise, *Control Systems Engineering*. Wiley, Hoboken, New Jersey, Fourth edition, 2008.

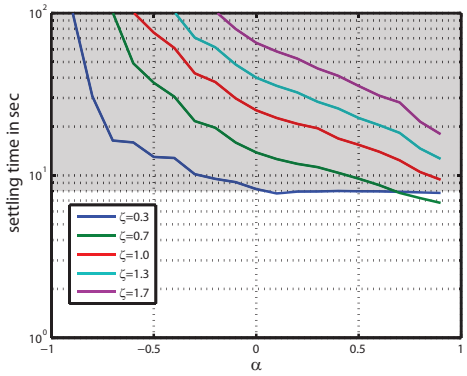

Fig. 14. Settling time as a function of α for several damping ratios

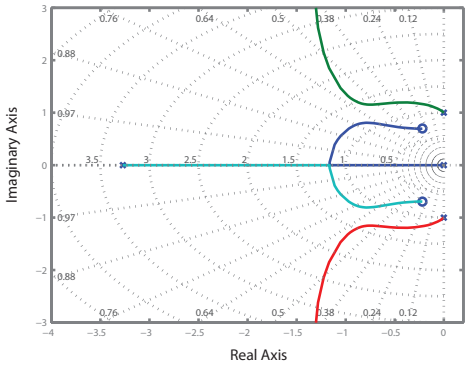

Fig. 15. Root locus of $P(s)C_{CPIL}(s)$

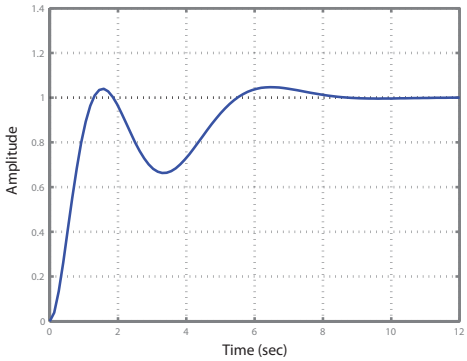

Fig. 16. Step response of $G_{CL,CPIL}$

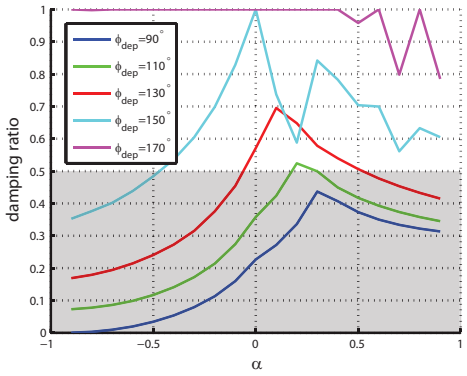

Fig. 17. Closed-loop damping ratio as a function of α for several values of ϕ_{dep}

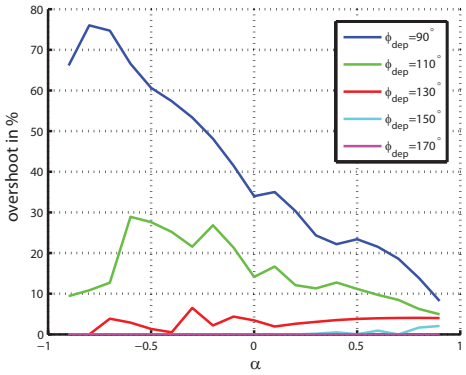

Fig. 18. Overshoot as a function of α for several values of ϕ_{dep}

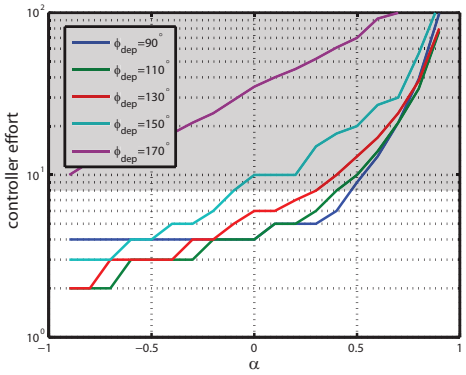

Fig. 19. Maximum controller effort as a function of α for several values of ϕ_{dep}

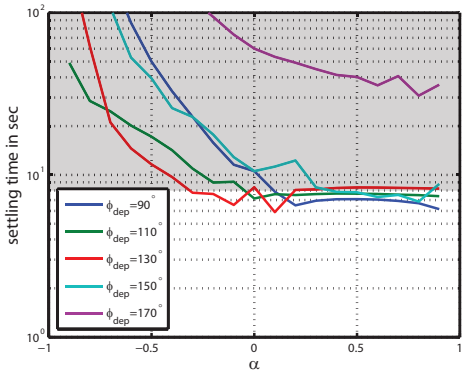

Fig. 20. Settling time as a function of α for several values of ϕ_{dep}